Progress In Electromagnetics Research, PIER 52, 321–333, 2005

ELECTROMAGNETIC SCATTERING FROM PERIODIC ARRAYS OF COMPOSITE CIRCULAR CYLINDER WITH INTERNAL CYLINDRICAL SCATTERERS

H. Toyama and K. Yasumoto

Department of Computer Science and Communication Engineering
Kyushu University 36
Fukuoka 812-8581, Japan

Abstract—A very efficient and accurate method to characterize the electromagnetic scattering from periodic arrays of two-dimensional composite cylindrical objects with internal eccentric cylindrical scatterers is presented, using the lattice sums formula and the aggregate T-matrix for cylindrical structures. The method is quite general and applies to various configurations of two-dimensional periodic arrays. The dielectric host cylinder per unit cell of the array can contain two or more eccentric cylindrical scatterers (we call them inclusions in this paper), which may be dielectric, conductor, gyrotropic medium, or their mixture with different sizes. The power reflection coefficients from one-layer or one-hundred-layered periodic arrays of composite cylinders with up to two inclusions have been numerically studied. The effect of the presence of inclusions on the properties of resonance peaks or the stopband's width will be discussed.

1. INTRODUCTION

Periodic dielectric or metallic structures have been a subject of continuing interest for applications to frequency selective or polarization selective devices in microwaves and optical waves. Various analytical or numerical techniques [1–3] have been developed to formulate the electromagnetic scattering from the periodic scatterers. Very recently, photonic bandgap structures (PBG's) [4, 5] in discrete periodic systems has received a growing attention, because they have many potential applications to narrow-band filters, high-quality resonant cavities, substrates for antennas and wave guides, and so forth. A periodic array of cylindrical scatterers is typical of discrete periodic structures. The frequency response of the array is characterized by the scattering properties per unit cell and the multiple scattering effects peculiar to the periodic arrangement of scatterers.

In this paper, we present a very accurate and efficient method for analyzing the electromagnetic scattering from periodic arrays of composite cylindrical objects, using the lattice sums technique [6] and the aggregate T-matrix [7] for a composite-cylinders system. The method is quite general and applies to a variety of configurations of periodic arrays of composite cylindrical objects. The dielectric host cylinder per unit cell can contain two or more eccentric cylinders, which may be dielectric, conductor, gyrotropic medium, or their mixtures with different dimensions. The scattered fields can be expressed in terms of the aggregate T-matrix for the composite cylinders located within a unit cell and the lattice sums characterizing the periodic arrangement of scatterers. The aggregate T-matrix is substantially changed by the inclusions' geometric parameters such as permittivity, size and location. As numerical examples, reflection characteristics of plane wave from one-layer or one-hundred-layered periodic arrays of composite cylinders with up to two inclusions for the fundamental and the first order space harmonics have been investigated. The effect of the presence of inclusions on the behaviour of reflection coefficient has been studied. It has been shown that in case of one inclusion per unit cell the resonance response in reflectance could be independent of polarizations. The inclusions would also refine directivity of the periodic arrays. Resonance peaks or stopband's width could be controllable by adjusting the inclusions' parameters for both polarizations.

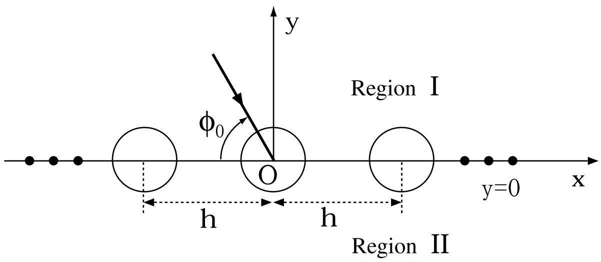

Figure 1. Cross section of a periodic array of cylindrical objects located at $y = 0$.

2. FORMULATION

First of all, we discuss the formulation for a periodic array consisting of homogeneous host cylinders using the lattice sums technique and the T-matrix approach. A periodic array of cylindrical objects is situated in a background medium with a wave number k_0 as shown in Fig. 1. The cylinders are infinite long, parallel to each other, and spaced with a distance h along the x axis on the plane $y = 0$, which separates the whole space into two semi-infinite regions assigned I and II, respectively. We consider the scattering of an electromagnetic plane wave whose direction of incidence is normal to the cylinder axis. The problem is then reduced to a two-dimensional one and may be treated separately for TM and TE waves relative to the z axis.

A plane wave with a unit amplitude is incident from the upper half-space $y > 0$. The wavevector forms an angle ϕ_0 relative to the x axis and its x component is $k_{x0} = k_0 \cos\phi_0$. The incident plane wave is expanded in terms of the cylindrical wave functions in a polar coordinate with the origin O at $(0, 0)$. The scattered field from the array is also expressed in the polar coordinate with the origin O at $(0, 0)$, using the lattice sums technique and a recursive algorithm for T-matrix. Let $\Psi(x, y)$ denote the E_z field for TM-wave problem and the H_z field in TE-wave problem, respectively. Using the recurrence formula and Fourier integral representation for Hankel functions, the scattered field can be finally obtained in terms of the Floquet space-harmonic waves in the xOy coordinate system. After several manipulations, the reflected field $\Psi_l^r(x, y)$ of the l-th space-harmonic in the upper half-space $y > 0$ and the corresponding transmitted field $\Psi_l^t(x, y)$ in the lower half-space $y < 0$ for downgoing incident plane wave are deduced as follows [8]:

$$\Psi_l^r(x, y) = \boldsymbol{u}_l^T \cdot \boldsymbol{a}^{sc} e^{i[k_{x,l}x + \kappa_l y]} \quad (l = 0, \pm 1, \pm 2, \cdots) \tag{1}$$

$$\Psi_l^t(x,y) = (\delta_{l,0} + \boldsymbol{v}_l^T \cdot \boldsymbol{a}^{sc}) e^{i[k_{x,l}x - \kappa_l y]} \tag{2}$$

with

$$\boldsymbol{u}_l = \left[\frac{2(-i)^m (k_{x,l} + i\kappa_l)^m}{h\kappa_l k_0^m}\right] \quad (m = 0, \pm 1, \pm 2, \cdots) \tag{3}$$

$$\boldsymbol{v}_l = \left[\frac{2(-i)^m (k_{x,l} - i\kappa_l)^m}{h\kappa_l k_0^m}\right] \tag{4}$$

$$\boldsymbol{a}^{sc} = (\boldsymbol{I} - \boldsymbol{T} \cdot \boldsymbol{L})^{-1} \cdot \boldsymbol{T} \cdot \boldsymbol{a}^{in} \tag{5}$$

$$\boldsymbol{a}^{in} = [i^m e^{im\phi_0}] \tag{6}$$

$$k_{x,l} = k_0 \cos\phi_0 + \frac{2l\pi}{h} \tag{7}$$

$$\kappa_l = \sqrt{k_0^2 - k_{x,l}^2} \tag{8}$$

where the vector quantities characterized by the index m are defined as column vectors, the superscript T indicates the transpose of vectors, $\boldsymbol{a}^{in}$ and $\boldsymbol{a}^{sc}$ represent the amplitude vectors of the incident plane wave and the scattered wave, respectively, based on field expansions in terms of cylindrical wave functions, $\boldsymbol{u}_l$ and $\boldsymbol{v}_l$ are vectors which transform the cylindrical waves to plane waves of the l-th space-harmonics, $\delta_{l,0}$ is the Kronecker's delta, and $\boldsymbol{I}$ is the unit matrix. In Eq. (5), $\boldsymbol{T}$ is the T-matrix of the isolated homogeneous cylinder whose center is located at the origin $(0,0)$, and $\boldsymbol{L}$ is a square matrix whose element L_{mn} is defined by

$$L_{mn} = S_{m-n}(k_0 h, \cos\phi_0) \tag{9}$$

$$S_n(k_0 h, \cos\phi_0) = \sum_{l=1}^{\infty} H_n^{(1)}(lk_0 h) e^{-ilk_0 h \cos\phi_0} + (-1)^n \sum_{l=1}^{\infty} H_n^{(1)}(lk_0 h) e^{ilk_0 h \cos\phi_0} \tag{10}$$

where $H_n^{(1)}$ is the n-th order Hankel function of the first kind. The semi-infinite sum $S_n(k_0 h, \phi_0)$ of the Hankel functions is the n-th order lattice sum [9]. Since the direct sum of Hankel functions in Eq. (10) converges very slowly, we calculate it by using the integral form referred to [6]. It follows from Eqs. (1) and (2) that the scattering process through the array plane is described in terms of the reflection coefficient r_l and the transmission coefficient f_l as

$$r_l = \boldsymbol{u}_l^T \cdot \boldsymbol{a}^{sc} \tag{11}$$

$$f_l = \delta_{l0} + \boldsymbol{v}_l^T \cdot \boldsymbol{a}^{sc} \tag{12}$$

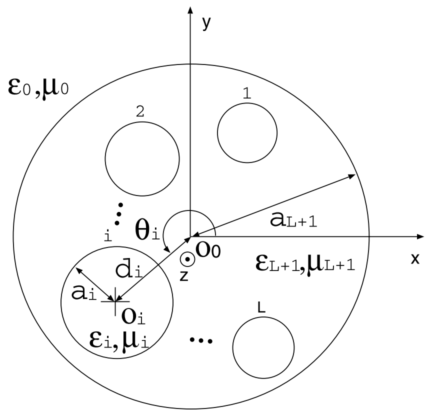

Figure 2. Cross sectional view of composite circular cylinders with L inclusions per unit cell. ε_i, μ_i, a_i, d_i and θ_i $(i = 1, 2, \cdots, L)$ denote the i-th inclusion's permittivity, permeability, radius, distance from the origin and angle measured from the x axis, respectively. Subscript $L+1$ denotes the host cylinder.

which relate the incident plane wave to the reflected and transmitted l-th space harmonics in the respective half-spaces.

3. AGGREGATE T-MATRIX

When a unit cell of the periodic array consists of a composite cylinder with multiple cylindrical inclusions eccentrically located inside the host cylinder, we can obtain the solution by combining both the lattice sums related to the periodic arrangement and the aggregate T-matrix [7] which characterizes the scattering properties of the whole cylindrical elements located within a unit cell. Let us consider a composite host cylinder with L-cylindrical inclusions, in general, as shown in Fig. 2. Provided that each inclusion is a circular cylindrical object and the T-matrix of each inclusion in isolation could be calculated, we summarize here the expressions for the aggregate T-matrix of the composite host cylinder with L inclusions in the unit cell for both TM and TE wave [10].

$$\begin{aligned}\boldsymbol{T}_{L+1} &= -[\eta_0 \boldsymbol{H}_0' - \eta_{L+1} \boldsymbol{F}'_{L+1} \cdot \boldsymbol{F}_{L+1}^{-1} \cdot \boldsymbol{H}_0]^{-1} \\ &\quad \times [\eta_0 \boldsymbol{J}_0' - \eta_{L+1} \boldsymbol{F}'_{L+1} \cdot \boldsymbol{F}_{L+1}^{-1} \cdot \boldsymbol{J}_0] \quad \text{for TM wave} \quad (13)\end{aligned}$$

$$\begin{aligned}\boldsymbol{T}_{L+1} &= -[\eta_{L+1} \boldsymbol{H}_0' - \eta_0 \boldsymbol{F}'_{L+1} \cdot \boldsymbol{F}_{L+1}^{-1} \cdot \boldsymbol{H}_0]^{-1} \\ &\quad \times [\eta_{L+1} \boldsymbol{J}_0' - \eta_0 \boldsymbol{F}'_{L+1} \cdot \boldsymbol{F}_{L+1}^{-1} \cdot \boldsymbol{J}_0] \quad \text{for TE wave} \quad (14)\end{aligned}$$

$$\boldsymbol{F}_{L+1} = \boldsymbol{J}_{L+1} + \boldsymbol{H}_{L+1} \cdot \boldsymbol{T}_L \tag{15}$$

$$\boldsymbol{F}'_{L+1} = \boldsymbol{J}'_{L+1} + \boldsymbol{H}'_{L+1} \cdot \boldsymbol{T}_L \tag{16}$$

$$\boldsymbol{T}_L = \sum_{i=1}^{L} \boldsymbol{\beta}_{0,i} \cdot \boldsymbol{T}_{i(L)} \cdot \boldsymbol{\beta}_{i,0} \tag{17}$$

with

$$\boldsymbol{J}_i = [J_m(k_i\, a_{L+1})\delta_{m,m'}],$$

$$\boldsymbol{J}'_i = [J'_m(k_i\, a_{L+1})\delta_{m,m'}] \quad (i=0,\, L+1) \tag{18}$$

$$\boldsymbol{H}_i = [H_m^{(1)}(k_i\, a_{L+1})\delta_{m,m'}], \quad \boldsymbol{H}'_i = [H_m^{(1)'}(k_i\, a_{L+1})\delta_{m,m'}] \tag{19}$$

$$k_i = \omega\sqrt{\varepsilon_i \mu_i}, \quad \eta_i = \sqrt{\varepsilon_i/\mu_i}, \tag{20}$$

where $\delta_{m,m'}$ is the Kronecker's delta, J_n is the n-th order Bessel function, $H_m^{(1)}$ is the m-th order Hankel function of the first kind, and the prime on the Bessel and Hankel functions denotes their derivatives with respect to the indicated arguments. Subscript $L+1$ denotes the host cylinder. In Eq. (17), $\boldsymbol{T}_L$ represents the aggregate T-matrix for the L inclusions inside the host cylinder. It can be derived from a recursive algorithm, i.e., the aggregate T-matrix for L inclusions is calculated from both the aggregate T-matrix for $L-1$ inclusions and the L-th inclusion's isolated T-matrix [7, 10]. $\boldsymbol{T}_{i(L)}$ is the T-matrix for the i-th cylinder in the presence of L cylinders in the host medium of infinite extent, and $\boldsymbol{\beta}_{i,j}$ is the translation matrix [7] for the regular part of cylindrical harmonics between the i and j coordinates.

Thus, in case when there are many cylindrical inclusions eccentrically located in the host cylinder in a unit cell as shown in Fig. 3, we can easily obtain the solution by substituting the aggregate T-matrix Eq. (13) or Eq. (14) alternatively into the T-matrix in the right hand side of Eq. (5).

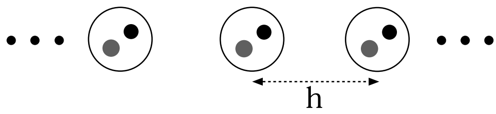

Figure 3. Cross section of a periodic array of composite cylindrical objects with internal scatterers.

4. MULTILAYERED SYSTEM

When the periodic array of the composite dielectric cylinders is multilayered as shown in Fig. 4, it constitutes a two-dimensional

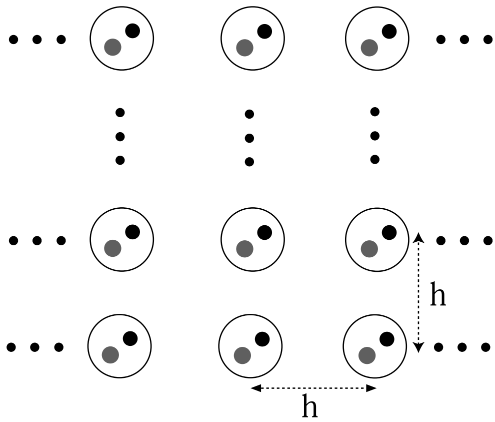

Figure 4. Cross section of a square lattice periodic array of composite cylindrical objects with internal scatterers.

photonic band gap structure. In the layered system, the multiple interaction of space-harmonics scattered from each of array layers modifies the frequency response and the photonic bandgaps or stopbands are formed in which any electromagnetic wave propagation is forbidden within a fairly large frequency range. In this paper, we have employed an accurate and efficient method for analyzing the electromagnetic scattering from the multilayered periodic arrays of circular cylinders, using the combination of the generalized reflection and transmission matrices [11] and the lattice sums technique discussed above. We have omitted to describe the details of the formulation of generalized reflection and transmission matrices, however, please see the reference [12].

5. NUMERICAL EXAMPLES

The reflection characteristics of periodic arrays of circular dielectric cylinders with up to two cylindrical inclusions have been numerically studied. Although a substantial number of numerical examples could be generated with the accuracy of energy-conservation errors less than 10^{-6}, we present in this paper the most fundamental results. Figure 5 illustrates the power reflection coefficient of the fundamental and the first order space harmonics for the normal incidence of both TM and TE wave with incident angle $\phi_0 = 90°$ as a function of normalized frequency h/λ_0 in case of homogeneous host cylinder. In the figure, ${}^{TM}R_\nu$ and ${}^{TE}R_\nu$ denote the reflection coefficients of the ν-th space

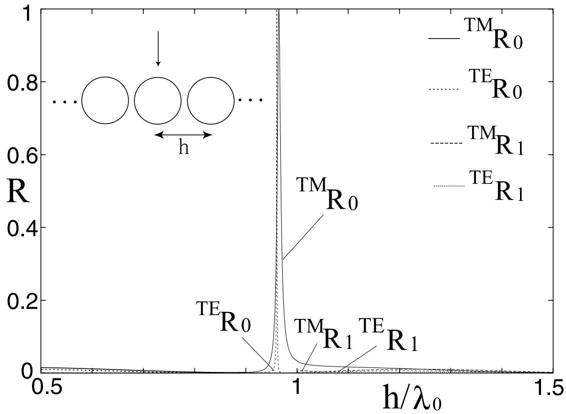

Figure 5. Power reflection coefficient of the lowest three space harmonics versus non-dimensional frequency h/λ_0 in case of homogeneous host cylinder for both TM and TE waves, where $a_1 = 0.3h$, $\varepsilon_1 = 1.5\varepsilon_0$, and $\phi_0 = 90°$.

harmonic for TM wave and TE wave, respectively. R_{-1} ($= R_1$) is omitted here because of the symmetric profile with respect to the y axis. Sharp resonances of both fundamental TM and TE wave have been seen near the frequency $h/\lambda_0 = 0.96$. This resonance profile is closely viewed in Fig. 6(a) and has been compared with the case of a composite cylinder with a coaxial dielectric inclusion shown in Fig. 6(b), where perfect coincidence of resonance has been observed at the same frequency for both TM and TE wave. We have obtained these parameters of Fig. 6(b) as slightly changing the inclusion's permittivity, by using the fact that TM wave whose electric field component E_z is parallel to the cylinders' axes could be more sensitive to change of the inclusion's permittivity than TE wave. At the resonance frequency $h/\lambda_0 = 0.9605$ in Fig. 6(b) the dependence of reflection coefficient on the incident angle has been examined and graphically plotted in Fig. 7. It is very interesting to see a sharp directivity just around $\phi_0 = 90°$ in Fig. 7(a), which is closely viewed in Fig. 7(b). The reflectance of this periodic array has a very narrow directivity with respect to the incident angle.

Figure 8(a) and 8(b) illustrate the power reflection coefficient of one-layer composite periodic arrays with two inclusions per unit cell versus normalized frequency h/λ_0 for TM and TE wave, respectively, where $a_1 = a_2 = 0.16h$, $d_1 = d_2 = 0.24h$, $\varepsilon_1 = \varepsilon_2 = 2.0\varepsilon_0$, $\theta_2 = \theta_1 + 180°$, $a_3 = 0.48h$, $\varepsilon_3 = 1.5\varepsilon_0$, and $\phi_0 = 90°$. The two inclusions which have same size and permittivity are located symmetrically with respect

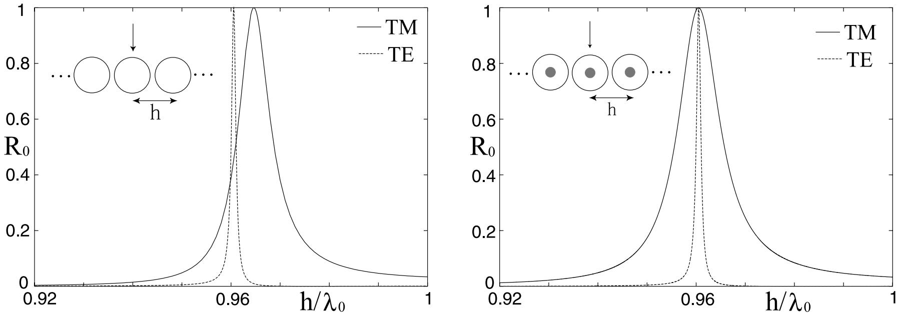

(a) (b)

Figure 6. Comparison of power reflection coefficient of the fundamental space harmonics versus non-dimensional frequency h/λ_0 for both TM and TE waves without inclusion (a), where the parameters are the same as in Fig. 5, with the case of coaxial dielectric inclusion (b), where $a_1 = 0.027h$, $d_1 = 0$, $\varepsilon_1 = 3.75\varepsilon_0$, $a_2 = 0.3h$, $\varepsilon_2 = 1.5\varepsilon_0$, and $\phi_0 = 90°$.

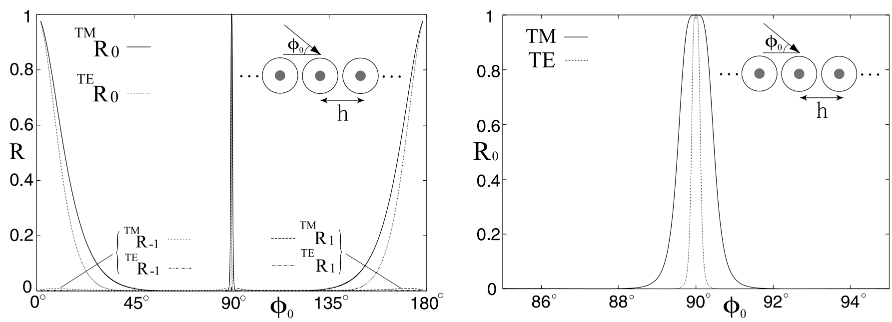

(a) (b)

Figure 7. Power reflection coefficient versus incident angle ϕ_0 for both TM and TE waves, where the geometric parameters are the same as in Fig. 6(b) and the frequency $h/\lambda_0 = 0.9605$. Fig. 7(a) is closely viewed in Fig. 7(b).

to the center of the host cylinder, and rotate from the x-axis plane ($\theta_1 = 0°$) to the y-axis plane ($\theta_1 = 90°$) as keeping the geometrical symmetricity ($\theta_2 = \theta_1 + 180°$). In this figure, solid lines show the results for the case without inclusions. Dashed line, short dashed line and dotted line show the results for the case of two inclusions with $\theta_1 = 0°$, $\theta_1 = 45°$ and $\theta_1 = 90°$, respectively. When the rotation angle θ_1 changes from $\theta_1 = 0°$ to $90°$, in case of two inclusions

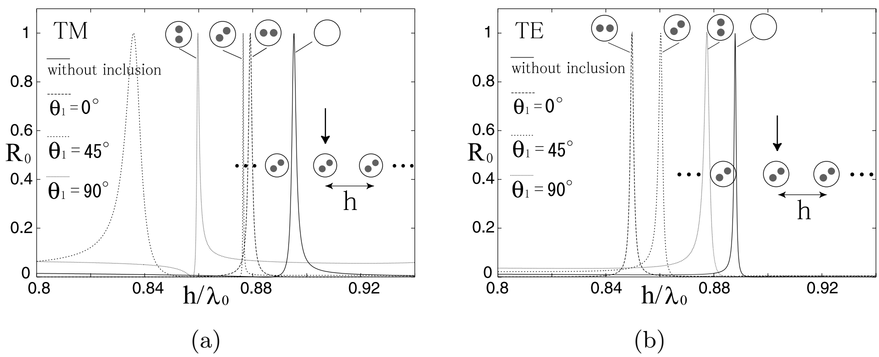

Figure 8. Power reflection coefficient of the fundamental space harmonics versus non-dimensional frequency h/λ_0 for one-layer periodic arrays of composite cylinders with two inclusions, where $a_1 = a_2 = 0.16h$, $d_1 = d_2 = 0.24h$, $\varepsilon_1 = \varepsilon_2 = 2.0\varepsilon_0$, $\theta_2 = \theta_1 + 180°$, $a_3 = 0.48h$, $\varepsilon_3 = 1.5\varepsilon_0$, and $\phi_0 = 90°$. (a) TM wave and (b) TE wave.

the resonance peak for TM wave shifts from $h/\lambda_0 = 0.88$ to lower frequency $h/\lambda_0 = 0.86$, whereas those characteristics for TE wave shift from $h/\lambda_0 = 0.85$ to higher frequency $h/\lambda_0 = 0.88$. The figures vividly show that the resonance frequency of the composite periodic arrays could be controllable by the slight change of the inclusions' geometrical parameters.

Using the same parameters for one-layer as in Fig. 8, frequency response for one-hundred-layered square lattice composite periodic arrays has been examined and graphically plotted in Fig. 9(a) and Fig. 9(b) for TM and TE wave, respectively. In the figures, solid lines, dashed lines and dotted lines indicate the power reflection coefficients in case of two inclusions, whose rotation angles are $\theta_1 = 0°$, $\theta_1 = 45°$ and $\theta_1 = 90°$, respectively. A perfect stopband has been observed from $h/\lambda_0 = 0.41$ to 0.43 for both TM and TE waves. It is noticeable that the stopband's width is gradually narrowing while the inclusions are rotating from $\theta_1 = 0°$ to $\theta_1 = 90°$, and the stopband's width in case of $\theta_1 = 90°$ is nearly half of the case of $\theta_1 = 0°$ for both TM and TE waves.

Frequency response for one-hundred-layered periodic arrays of composite cylinders with higher permittivities than in Fig. 9, has been demonstrated in Fig. 10. The permittivities of inclusions and the host cylinder are $\varepsilon_1 = \varepsilon_2 = 2.5\,\varepsilon_0$ and $\varepsilon_3 = 2.0\,\varepsilon_0$, whereas other geometrical parameters are the same. In this case, the stopband has been observed in lower frequency region than in Fig. 9, and its width

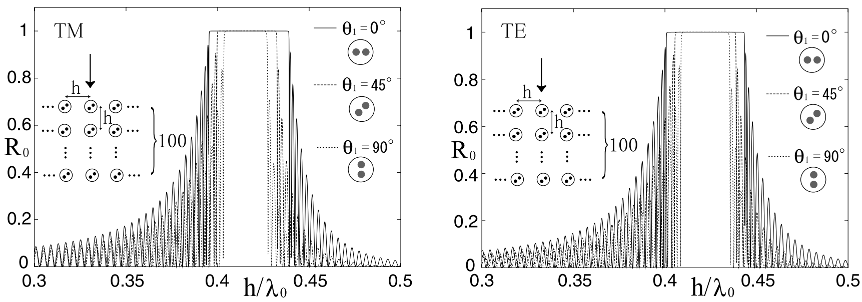

(a) (b)

Figure 9. Power reflection coefficient of the fundamental space harmonics versus non-dimensional frequency h/λ_0 for one-hundred-layered square lattice periodic arrays of composite cylinders with two inclusions, where $a_1 = a_2 = 0.16h$, $d_1 = d_2 = 0.24h$, $\varepsilon_1 = \varepsilon_2 = 2.0\varepsilon_0$, $\theta_2 = \theta_1 + 180°$, $a_3 = 0.48h$, $\varepsilon_3 = 1.5\varepsilon_0$, and $\phi_0 = 90°$. (a) TM wave and (b) TE wave.

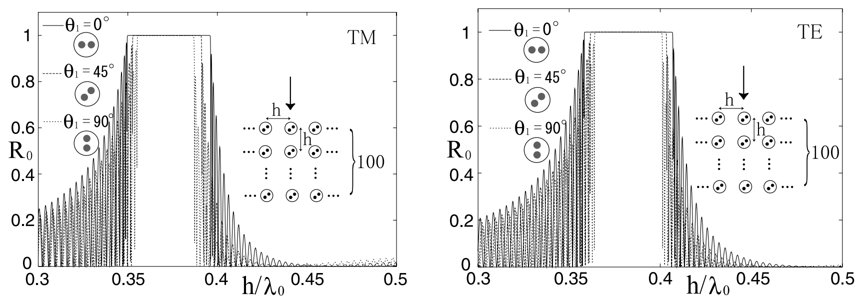

(a) (b)

Figure 10. Power reflection coefficient of the fundamental space harmonics versus non-dimensional frequency h/λ_0 for one-hundred-layered square lattice periodic arrays of composite cylinders with two inclusions, where parameters are the same as in Fig. 9 except $\varepsilon_1 = \varepsilon_2 = 2.5\varepsilon_0$ and $\varepsilon_3 = 2.0\varepsilon_0$. (a) TM wave and (b) TE wave.

has also become narrower when the two inclusions rotate from $\theta_1 = 0°$ to $\theta_1 = 90°$. From Fig. 9 and Fig. 10, it follows that stopband's width and its frequency region for the multilayered periodic arrays with composite cylinders could be controllable by adjusting the inclusions' permittivities and geometrical parameters for both polarizations.

6. CONCLUSION

We have presented a rigorous method for the electromagnetic scattering from periodic arrays of two-dimensional composite circular cylinders with internal cylindrical scatterers, using the lattice sums technique and the T-matrix approach. The proposed method has been used to analyze the reflection characteristics of plane waves from one-layer or one-hundred-layered periodic arrays of the composite cylinders with up to two internal scatterers. The effects of the presence of internal scatterers on the behaviour of reflectance characteristics for various configurations of periodic structures have been investigated. It has been shown that the resonance properties and the stopband's width for both polarizations could be controllable by properly adjusting the permittivities and the geometrical parameters of the internal scatterers.

REFERENCES

1. Twersky, V., "On scattering of waves by the infinite grating of circular cylinders," *IRE Trans. Antennas Propagat.,* Vol. 10, 737–765, Nov. 1962.
2. Petit, R. (ed.), *Electromagnetic Theory of Grating,* Springer-Verlag, Berlin, 1980.
3. Roussel, H., C. W. Chew, F. Jouvie, and W. Tabbara, "Electromagnetic scattering from dielectric and magnetic gratings of fibers — A T-matrix solution," *J. Electromagn. Waves and Appl.,* Vol. 10, No. 1, 109–127, 1996.
4. Scherer, A., T. Doll, E. Yablonovitch, H. O. Everitt, and J. A. Higgins (eds.), "Special section on electromagnetic crystal structures, design, synthesis, and applications," *J. Lightwave Technol.,* Vol. 17, No. 11, 1928–2207, 1999.
5. —–, "Mini-special issue on electromagnetic crystal structures, design, synthesis, and applications," *IEEE Trans. Microwave Theory Tech.,* Vol. 47, No. 11, 2057–2150, 1999.
6. Yasumoto, K. and K. Yoshitomi, "Efficient calculation of lattice sums for free-space periodic green's function," *IEEE Trans. Antennas Propagat.,* Vol. 47, No. 6, 1050–1055, 1999.
7. Chew, C. W., *Waves and Fields in Inhomogeneous Media*, Van Nostrand Reinhold, New York, 1990.
8. Kushta, T. and K. Yasumoto, "Electromagnetic scattering from periodic arrays of two circular cylinders per unit cell," *Progress In Electromagnetics Research,* PIER 29, 69–85, 2000.

9. Nicorovici, A. N. and C. R. McPhedran, "Lattice sums for off-axis electromagnetic scattering by grating," *Phys. Rev. E.,* Vol. 50, No. 4, 3143–3160, 1994.
10. Toyama, H., K. Yasumoto, and T. Iwasaki, "Electromagnetic scattering from a dielectric cylinder with multiple eccentric cylindrical inclusions," *Progress In Electromagnetics Reseach,* PIER 40, 113–129, 2003.
11. Yasumoto, K., "Generalized method for electromagnetic scattering by two-dimensional periodic discrete composites using lattice sums," *Proceedings of 2000 International Conference on Microwave and Millimeter Wave Technology*, P-29-P-34, Sep. 2002.
12. Yasumoto, K., H. Toyama, and T. Kushta, "Accurate analysis of two-dimensional electromagnetic scattering from multilayered periodic arrays of circular cylinders using lattice sums technique," *IEEE Transactions on Antennas and Propagation*, Vol. 52, No. 10, 2603–2611, Oct. 2004.

Hiroshi Toyama was born in Fukuoka, Japan, on May 13 1966. He is presently a Ph.D. student of Department of Computer Science and Communication Engineering at Kyushu University. He received B.S. and M.S. in 1990 and in 1992, respectively, from Kyushu University. He worked for NEC Corporation in Tokyo. His current research interests include electromagnetic scattering from discrete periodic structures.

Kiyotoshi Yasumoto was born in Oita, Japan, on March 8, 1945. He received the B.E., M.E., and D.E. degrees in communication engineering from Kyushu University, Fukuoka, Japan, in 1967, 1969, and 1977, respectively. In 1969, he joined at the Faculty of Engineering of Kyushu University, where he is now a Professor of the Department of Computer Science and Communication Engineering. He was a Visiting Professor of the Department of Electrical and Computer Engineering, University of Wisconsin-Madison in 1989. His research interests are in electromagnetic wave theory, microwave and optical waveguides, and numerical analysis. Dr. Yasumoto is a fellow of Optical Society of America and Chinese Institute of Electronics, a senior member of IEEE, and a member of IEICE Japan, IEE Japan and Electromagnetic Academy.